


The three-dimensional speckle tracking echocardiography in distinguishing between ischaemic and non-ischaemic aetiology of heart failure

Marianna Vachalcova^{1,2}, Gabriel Valočík^{1,2}, Marián Kurečko^{1,2}, Julia Grapsa³, Viktória Ali Taha⁴, Peter Michalek^{5,6}, Monika Jankajová^{1,2}, František Sabol^{1,2}, Lucia Kubikova^{1,2}, Marek Orban^{6,7}, Tomas Uher^{9,10} and Allan Böhm^{7,8,9*} 

¹East Slovak Institute of Cardiovascular Diseases, Kosice, Slovakia; ²Faculty of Medicine, Pavol Jozef Šafárik University, Kosice, Slovakia; ³Cardiology Department, Guys and St Thomas NHS Hospitals, London, UK; ⁴University of Prešov, Prešov, Slovakia; ⁵University Hospital of St. Cyril and Methodius, Bratislava, Slovakia; ⁶Faculty of Medicine, Comenius University, Bratislava, Slovakia; ⁷National Institute of Cardiovascular Diseases, Bratislava, Slovakia; ⁸Faculty of Medicine, Slovak Medical University, Bratislava, Slovakia; ⁹Academy-Research Organization, Bratislava, Slovakia; ¹⁰Internal Department, Malacky Hospital, Malacky, Slovakia

Abstract

Aims The aim of this pilot study was to compare selected three-dimensional speckle tracking echocardiography (3D STE) parameters in patients with ischaemic and non-ischaemic aetiology of heart failure (HF) and to identify indices that can differentiate the two pathologies.

Methods and results Forty patients with left ventricular ejection fraction (LVEF) $\leq 40\%$ were included to the study: 20 patients (age 63 ± 9.0 years, LVEF $29.0 \pm 11.3\%$) with ischaemic cardiomyopathy and 20 patients (age 64.0 ± 11.0 years, LVEF $27.3 \pm 7.5\%$) with non-ischaemic cardiomyopathy. All patients underwent two-dimensional (2D) and three-dimensional (3D) transthoracic echocardiography. Standard echocardiographic parameters, global longitudinal strain, and rotational parameters of left ventricle (LV) were assessed using 3D speckle tracking (3D STE). There were no differences in standard and STE parameters between the two groups. Among rotational parameters, the LV apical rotation ($4.9 \pm 3.5^\circ$ vs. $2.3 \pm 2.4^\circ$, $P = 0.0022$) was significantly higher in patients with ischaemic HF. Among all echocardiographic parameters, a cut-off value of 3.28° (area under the curve 0.78; 95% confidence interval, 0.62 to 0.93) was able to distinguish the ischaemic and non-ischaemic aetiology of HF with a sensitivity of 80% and specificity of 75%.

Conclusions This is the first study that compares 3D STE parameters between patients with ischaemic and non-ischaemic cardiomyopathy. It was proved that the apical rotation was significantly higher in patients with ischaemic cardiomyopathy. Our findings suggest that 3D STE might be useful in non-invasive differentiation between ischaemic and non-ischaemic aetiology of HF.

Keywords Apical rotation; 3D echocardiography; Speckle tracking echocardiography; Heart failure aetiology; Coronary artery disease; Non-ischaemic cardiomyopathy

Received: 27 November 2019; Revised: 10 April 2020; Accepted: 7 May 2020

*Correspondence to: Allan Böhm, National Institute of Cardiovascular Diseases, Pod Krásnou hôrkou 7185, Bratislava 83101, Slovakia.
Email: allan.bohm@gmail.com

Introduction

Echocardiography is the first line imaging modality for heart failure (HF) diagnosis and treatment-effect monitoring. It enables us to evaluate myocardial deformity and thereby the assessment of global and regional functions. There has been a technological transition of myocardial deformation analysis

from tissue Doppler imaging to two-dimensional (2D)¹ and the latest three-dimensional (3D) speckle tracking echocardiography (STE) methods.²

Despite significant improvements in available HF treatment regimens, the 12-month all-cause mortality of 17% in hospitalized patients and 7% in stable or ambulatory patients remains high. Ischaemic heart disease is the most common

cause of HF and is associated with worse prognosis compared with patients with non-ischaemic aetiology.^{3,4} Therefore, taken into consideration the potential specific treatment strategy of ischaemic HF, it is important to differentiate it from non-ischaemic HF.⁵

Regarding prognosis and different therapeutic approaches, HF aetiology is usually specified with cardiac magnetic resonance (CMR), computed tomography, or invasive coronary angiography.^{6–8}

The 3D STE with its capability to analyse the myocardial mechanics is a cost-effective imaging modality. Its applicability and clinical relevance in the differentiation between ischaemic and non-ischaemic cardiomyopathy (NICM) lack sufficient data.

For that purpose, we designed a study where we analysed selected 3D STE parameters and their difference between patients with ischaemic cardiomyopathy (ICM) and NICM in order to find potential parameters capable of identifying HF aetiology.

Methods

Study population

We prospectively recruited 40 consecutive patients referred to the Cardiology Department of East Slovakian Institute of Cardiovascular Disease who underwent transthoracic echocardiography (TTE) and coronary angiography, with New York Heart Association functional class II or III symptomatic HF, left ventricular ejection fraction $\leq 40\%$ with wall motion abnormality in the anterolateral and apical wall, and good quality of echocardiographic recordings.

The inclusion criteria for the ICM group were ischaemic heart disease defined as prior history of myocardial infarction or coronary revascularization or $\geq 75\%$ stenosis of at least one epicardial coronary artery. The inclusion criteria for NICM group were no history of myocardial infarction, ischaemic heart disease, and absence of epicardial coronary artery stenosis $\geq 50\%$. Patients with left ventricular aneurysm, congenital heart disease, hypertrophic cardiomyopathy, restrictive cardiomyopathy, pericardial diseases, significant valvular disease, uncontrolled heart rate, left bundle branch block, implanted pacemaker, HF due to untreated valvular heart disease, or with significant renal dysfunction (estimated glomerular filtration rate < 30 mL/min/1.73 m²) were excluded from both groups.

All procedures performed were in accordance with the ethical standards of the Helsinki Declaration from 1975. Approval was given by the local institutional ethical committee. All enrolled patients provided written informed consent.

Echocardiographic protocol

The 2D and 3D TTE were performed in each patient, using Siemens SC2000 ultrasonograph with 2.5–3.75 MHz and 4Z1c transducer (Siemens Medical Solutions, Inc., Mountain View, California, United States).

The 3D STE was used for the assessment of the left ventricle (LV) global longitudinal strain and rotation parameters. For Doppler and 3D STE measurements, three cycles in sinus rhythm and five cycles in atrial fibrillation were averaged. The average frame rate of the 3D STE images was 18 Hz.

The echocardiographic protocol adhered to the recommendations for chamber quantification of the American Society of Echocardiography and the European Association of Cardiovascular Imaging and to the expert consensus document of the European Association of Cardiovascular Imaging.^{9,10}

The echocardiographic variables were analysed offline using the Image Arena Workstation (Tom Tec, Munich, Germany). Measurements were performed by a senior reader certified in echocardiography and blinded to the patients' clinical data and outcomes.

Left ventricular ejection fraction, end diastolic, and end systolic volumes were assessed by a modified biplane Simpson's rule. LV mass and its indexed values (indexed to body surface area in square metre) were calculated using the formula by Devereux *et al.*¹¹

LV diastolic filling was assessed by pulsed wave Doppler echocardiography from trans-mitral flow. The peak E wave velocity (early filling wave), transmitral Doppler E wave deceleration time, and peak A wave velocity (late filling wave) were measured. Myocardial velocity of the basal interventricular septum was assessed by pulsed wave tissue Doppler echocardiography in systole (Sm) and diastole (Em). E/Em ratio was calculated as a measure of left ventricular filling pressure. Left atrial volume was measured by the biplane Simpson's method in apical four-chamber and two-chamber views and indexed to body surface area.

Out of 3D data set, five 2D cross-sectional planes were generated for tracking the endocardium and epicardium: an apical four-chamber plane, an orthogonal two-chamber plane, and a three short-axis planes (near the apex, mid-level, and the base of the LV). LV endocardium and epicardium were traced automatically by the 3D wall motion tracking software. Verification and manual adjustment were performed on a basis of the 2D cross-sectional planes where needed. LV was divided by the software into 16 segments to assess the magnitude and timing of the regional myocardial deformation according to the American Society of Echocardiography and the European Association of Cardiovascular Imaging.⁹ The 3D wall motion tracking enabled simultaneous determination of global longitudinal, circumferential, and radial systolic strain as well as rotation of all the 16 LV segments. The average rotational magnitude of the six basal

(anterior, antero-septal, infero-septal, inferior, infero-lateral, and antero-lateral) and four apical (septal, inferior, lateral, and anterior) segments was calculated. LV twist was derived from the systolic rotation of the apical relative to the basal segments. Division of the LV twist by the distance between the apical and basal segments yielded torsion.

To assess intra-observer reproducibility, the same observer blinded to the patients' clinical data and outcomes performed the analysis on 10 random patients at an interval of several months to avoid recall bias. To assess inter-observer reproducibility, analysis was performed on the same patients by a second observer who was blinded to the patients' data and the results of the first observer.

Statistical analysis

Continuous variables were expressed as means \pm standard deviation. Categorical variables were expressed as *N* (%). Normality of data was assessed using a Shapiro–Wilk test. Unpaired Student's *t*-test and Mann–Whitney were used to compare continuous variables as appropriate. Fisher's exact test was used for categorical data. Receiver operating characteristic (ROC) curve together with respective values of sensitivity, specificity, and accuracy at various cut-off levels of the selected parameter were calculated to evaluate the diagnostic performance. The estimates are presented together with 95% confidence intervals. Intra-observer and inter-observer reproducibility were assessed using

intra-class correlation coefficient. The effect of explanatory variables was evaluated using logistic regression analysis. $P \leq 0.05$ was considered statistically significant. Data were analysed using StatsDirect statistical software version 3.1.22 (<http://www.statsdirect.com>).

Results

In total, 40 patients, 34 male patients and 6 female patients with a mean age of 63 ± 10 years were enrolled into this study. Twenty consecutive patients in the ICM group and 20 consecutive patients in the NICM group, respectively. *Table 1* shows the baseline demographics between the ICM and NICM patients. There were no significant differences between the groups in terms of age, body mass index, blood pressure, heart rhythm, baseline New York Heart Association status, cardiovascular comorbidities, or concomitant drug therapy. *Table 2* shows volumetric data and functional parameters for the ICM and NICM groups. There were no differences in standard TTE and STE parameters among patients with ischaemic and non-ischaemic aetiology, including global longitudinal strain (-8.0 ± 4.5 vs. $-8.4 \pm 2.9\%$, $P = 0.731$). Significant difference was found in apical LV rotation (AR). ICM patients had higher CR ($4.9 \pm 3.5^\circ$ vs. $2.3 \pm 2.4^\circ$, $P = 0.0022$) compared with the NICM group (*Figure 1*). *Figures 2 and 3* show 3D echocardiographic assessment of LV parameters in ICM and NICM, respectively.

Table 1 Baseline characteristics

	ICM ¹²	NICM ¹²	<i>P</i> value
Age (years)	62.55 \pm 9.04	64.00 \pm 10.95	0.65
Sex (male) (%)	19 (95)	15 (75)	0.18
SBP (mmHg)	135.61 \pm 21.82	124.75 \pm 15.60	0.09
DBP (mmHg)	81.28 \pm 13.72	77.50 \pm 15.94	0.44
Height (cm)	172.00 \pm 6.15	170.20 \pm 7.95	0.43
Weight (kg)	83.00 \pm 11.94	80.75 \pm 12.81	0.57
Body mass index (kg/m ²)	28.29 \pm 3.79	28.00 \pm 3.55	0.80
Heart rate (bpm)	74.90 \pm 14.49	73.90 \pm 12.89	0.89
DM. <i>n</i> (%)	9 (45)	6 (30)	0.51
Hypercholesterolemia (%)	12 (60)	6 (30)	0.11
Creatinine (umol/L)	115.21 \pm 20.79	116.50 \pm 30.91	0.88
AFib (%)	7 (35)	6 (30)	$P > 0.99$
NYHA class II (%)	3 (15)	2 (10)	$P > 0.99$
NYHA class III (%)	16 (80)	18 (90)	0.66
Beta blockers (%)	18 (90)	17 (85)	$P > 0.99$
ACEi/ARB (%)	18 (90)	13 (65)	0.13
Aldosterone antagonist (%)	14 (70)	9 (45)	0.20
Akinesia in ALAW (%)	5 (26)	3 (16)	0.46
Myocardial infarction (%)	3 (16)	0	Not applicable
PCI/CABG (%)	7 (35)	0	Not applicable

ACEi/ARB, angiotensin converting enzyme inhibitor/angiotensin receptor blocker; Afib, atrial fibrillation; ALAW, anterolateral and apical wall; CABG, coronary artery bypass grafting; DBP, diastolic blood pressure; DM, diabetes mellitus; ICM, ischaemic cardiomyopathy; NICM, non-ischaemic cardiomyopathy; NT-proBNP, N terminal pro b-type natriuretic peptide; NYHA, New York Heart Association; PCI, percutaneous coronary intervention; SBP, systolic blood pressure.

Data as mean \pm standard deviation or *n* (%).

Table 2 Volumetric data and functional parameters

	ICM (20)	NICM (20)	P value
LVAR, °	4.91 ± 3.48	2.29 ± 2.36	<i>P</i> < 0.01
LVBR, °	-2.21 ± 2.39	-2.80 ± 1.71	0.14
Twist, °	5.25 ± 4.51	3.48 ± 3.31	0.15
Torsion, °/cm	0.65 ± 0.59	0.43 ± 0.39	0.17
GLS, %	-7.99 ± 4.49	-8.40 ± 2.93	0.73
EF, %	29.03 ± 11.26	27.25 ± 7.52	0.56
EDV, mL	168.08 ± 52.83	170.83 ± 62.45	0.88
ESV, mL	120.45 ± 47.61	126.53 ± 55.29	0.84
LAV, mL	76.77 ± 45.88	67.35 ± 29.80	0.61
LAVI, mL/m ²	40.09 ± 25.52	37.32 ± 15.01	0.99
SDI, %	7.99 ± 4.19	9.83 ± 5.39	0.37
EDT, ms	167.06 ± 71.32	215.15 ± 114.84	0.13
E/A	1.61 ± 1.47	1.27 ± 1.17	0.28
E/Em	14.94 ± 9.16	12.84 ± 5.02	0.70

EDV, end-diastolic volume; EDT, E wave deceleration time; EF, ejection fraction; Em, tissue Doppler early diastolic myocardial velocity of the basal septum; ESV, endsystolic volume; GLS, global longitudinal strain; ICM, ischaemic cardiomyopathy; LAV, left atrial volume; LV AR, left ventricular apical rotation; LV BR, left ventricular basal rotation; NICM, non-ischaemic cardiomyopathy; SDI, systolic dyssynchrony index.

Data as mean ± standard deviation.

After adjustment for history of myocardial infarction and presence of akinesia in anterolateral and apical wall region, only apical rotation remained significantly associated with ICM (odds ratio: 1.54; *P* = 0.025; *Table 3*).

Based on the ROC analysis, the AR value of 3.28° had 80% sensitivity and 75% specificity for the prediction of HF aetiology (area under the curve 0.78, 95% confidence interval, 0.62–0.93; *Figure 4*).

Intra-class correlation coefficients of the intra-observer and inter-observer reproducibility for of the STE parameters were >0.9 (*Table 4*).

Discussion

Our pilot study is the first one to demonstrate that AR measured by 3D TTE is significantly different between ICM and NICM patients. Based on the best-case scenario ROC analysis, the cut-off value of 3.28° differentiated the ischaemic from the non-ischaemic HF aetiology.

For the study, we preferred 3D over 2D TTE. The 2D echocardiography has pre-specified imaging planes that show limited information from the whole LV myocardium unlike the 3D echocardiography, which has the ability to display all myocardial segments simultaneously in multi-level slices, offering a comprehensive assessment of the entire LV myocardial performance. Fixed 2D cutting planes lose speckles during frame-by-frame speckle tracking analysis during through-plane motion of the heart. In 3D STE, speckles of the entire myocardium are tracked omnidirectionally in 3D space and therefore out-of-plane motion speckle tracking errors are eliminated. 3D STE enables simultaneous and more accurate measurement of rotations in the basal and apical short-axis planes and the distance between the planes. Moreover, compared with 2D, 3D echocardiography has been shown to better correlate with CMR, which is recognized as the reference standard non-invasive technique for measurement of myocardial strain and rotational parameters.^{13,14}

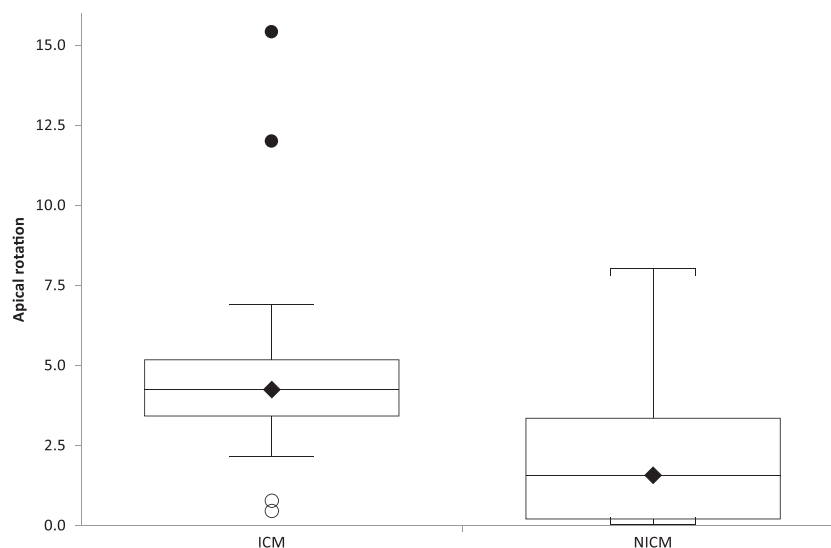
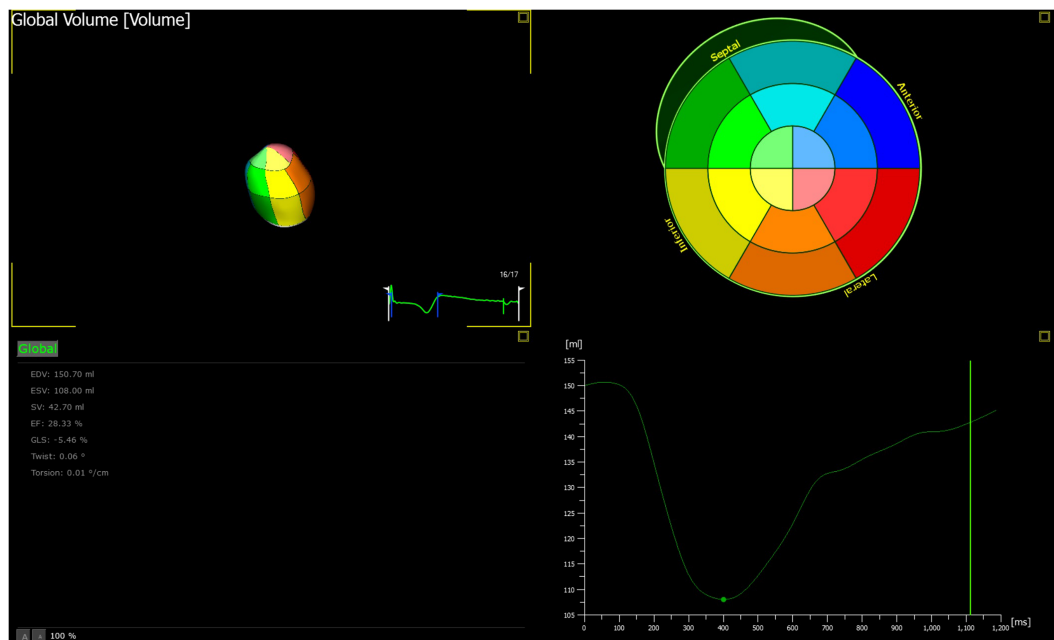
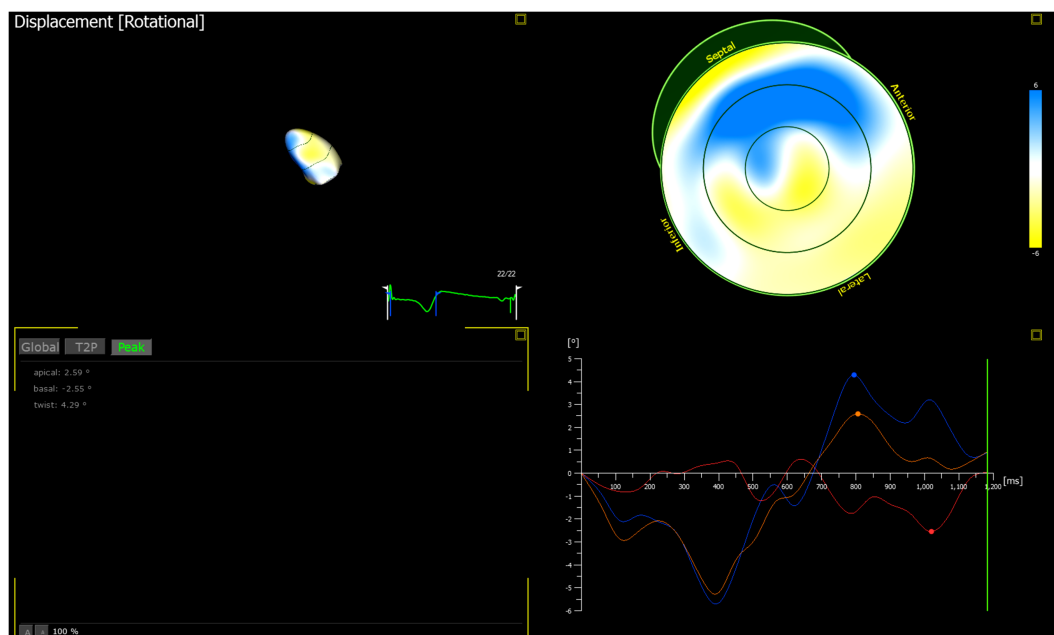
Figure 1 Box and whisker plot. ICH, ischaemic cardiomyopathy; NICM, non-ischaemic cardiomyopathy.

Figure 2 Three-dimensional echocardiographic assessment of left ventricular volumetric parameters in ischaemic cardiomyopathy.**Figure 3** Three-dimensional echocardiographic assessment of left ventricular rotational parameters in non-ischaemic cardiomyopathy. EDV, end diastolic volume; ESV, end systolic volume; SV, stroke volume; EF, ejection fraction; GLS, global longitudinal strain.

The LV consists of obliquely oriented muscle fibres that vary from a smaller radius, right-handed helix at the sub-endocardium to a larger radius, left-handed helix at the sub-epicardium. The functional consequence of this

three-dimensional helical structure is a cyclic systolic twisting deformation, resulting from clockwise basal rotation and anticlockwise apical rotation (as seen from the apex).¹⁵

Table 3 Multivariate analysis

	Odds ratio	(95% confidence interval)	P value
LVAR, °	1.54	(1.06–2.24)	0.025
MI	0.74	(0.28–55.54)	0.75
Akinesia in ALAW	3.96	(0.11–4.94)	0.30

ALAW, anterolateral and apical wall; LV AR, left ventricular apical rotation; MI, myocardial infarction.

Rotation is very important for clinical practice as it refers to the angular myocardial rotation in each short-axis plane around the LV longitudinal axis and is expressed in degrees or radians. By convention, anticlockwise rotation is assigned a positive value whereas clockwise rotation is given a negative value. During isovolumic contraction, an initial global anticlockwise rotation of the heart occurs, as can be seen from the cardiac apex. During ventricular ejection, the apex continues its anticlockwise rotation whereas the base rotates in a clockwise direction. In the isovolumic relaxation phase, the apex recoils rapidly with clockwise rotation to generate a steep decay of ventricular pressure and an active suction force. Untwisting of the LV is completed in early diastole.

Last but not least, twist is defined as the absolute apex-to-base difference in rotation and is expressed in degrees or radians. The direction of LV twist is determined by the sub-epicardial fibres. The ratio of the twist and LV length is torsion in degrees or radians per centimetre.¹⁶ Twist plays a

Table 4 Intra-observer and inter-observer reproducibility

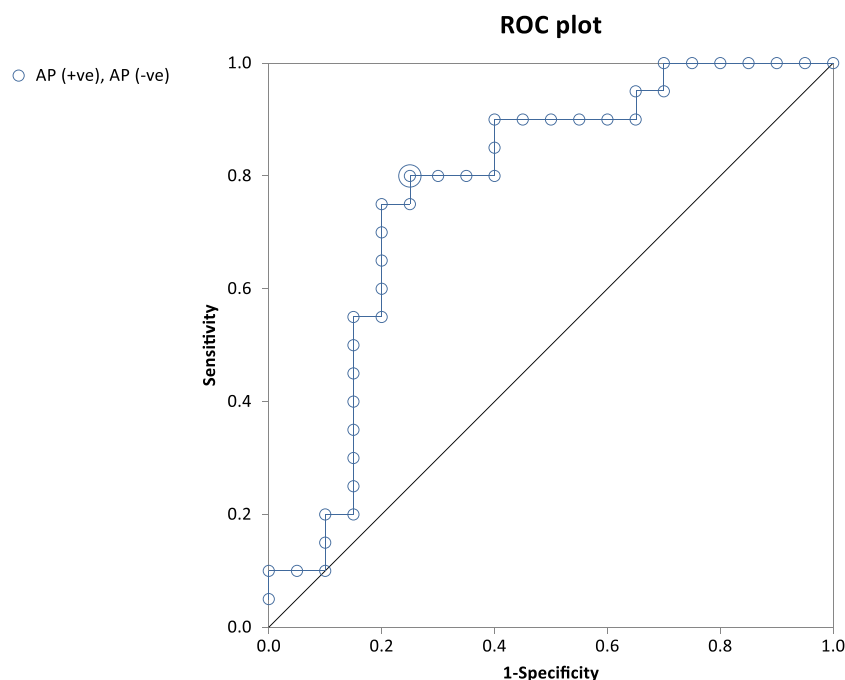
	ICC for intra-observer reproducibility	ICC for inter-observer reproducibility
LVAR, °	0.95	0.98
LVBR, °	0.99	0.99
Twist, °	0.96	0.93
Torsion, °/ cm	0.94	0.92
GLS, %	0.95	0.95

GLS, global longitudinal strain; ICC, intra-class correlation coefficient; LV AR, left ventricular apical rotation; LV BR, left ventricular basal rotation.

pivotal role in the mechanical efficiency of the heart, allowing that only 15% fibre shortening results in a 60% reduction of the LV volume.¹⁷

In coronary artery disease (CAD), loss of contraction of the counteracting subendocardial fibres will lead to dominant action of the sub-epicardial fibres and maintaining the direction of apical rotation. LV torsion impairs due to impaired basal rotation, whereas apical rotation does not impair at the same rate, suggesting a compensatory role.¹⁸

Kroeker *et al.*,¹⁹ using an optical device coupled to the LV apex in 16 open-chest dogs, found a decrease of LV apical rotation with ischaemia caused by occlusion of the left anterior descending coronary artery. In the first 10 s of occlusion, however, there was a paradoxical increase in LV apical

Figure 4 Receiver operating characteristic curve for the apical rotation.

rotation, which was attributed to isolated sub-endocardial ischaemia leading to loss of counteractive action of the sub-endocardial helix of myofibres.

In contrast to CAD, the patients with NICM have impairment of sub-endocardial and sub-epicardial myocardial layer. That leads to the loss of dynamic interaction between opposing oriented myocardial fibres and to the decrease in apical rotation, up to the change of its rotational direction. Therefore, the value of AR is lower compared with CAD. This finding is confirmed by Ojaghi Haghghi *et al.* trial.²⁰ The authors demonstrated that systolic torsion in NICM was characterized by an interruption of anticlockwise apical rotation before the systole termination. The size and shape of the LV are gradually changing with its remodelling, which also changes the rotational parameters.

Differentiating the ICM from the NICM is of paramount importance due to the different prognosis and treatment strategies.^{4,6} Coronary angiography is a gold standard method to diagnose the CAD. Despite its routine use in the clinical practice, it is time requirements, radiation load, and periprocedural complications that make it a complex examination with strict indications.¹² Patients without any significant coronary artery stenosis and without the detection of any other cause of ejection fraction reduction are usually diagnosed with NICM.¹⁵ On the other hand, gadolinium-enhanced magnetic resonance imaging is a powerful non-invasive technique to distinguish NICM from LV dysfunction related to CAD. It was demonstrated that patients with CAD or with documented recanalization after an occlusive coronary event or embolization from unstable plaque had sub-endocardial or trans-mural gadolinium enhancement that indicated the fibrosis in this area. Late gadolinium enhancement clearly distinguished patients without CAD, and it has been suggested that CMR is a suitable method to differentiate HF caused by CAD and NICM.²¹

CMR has significant limitations such as complex patient preparation requirement, long duration of the examination, costs, potential radiation load, and periprocedural complications make their routine use difficult. Therefore, 3D STE might be the new modality capable of replacing these labourious imaging methods in differential diagnosis between the ICM and NICM. According to our knowledge, the functional parameters of the ICM and NICM assessed by the 3D STE were not studied before, and this is the first demonstration of the 3D STE potential utility in differentiation between the ischaemic and non-ischaemic aetiology of the HF.

Limitations

The study has some limitations. The low spatial resolution of 3D wall motion tracking could affect the delineation of endocardial and epicardial layers and, in turn, the accuracy of tracking.

CAD is the cause of HF if a history of prior myocardial infarction, revascularization (surgical or percutaneous) is present, or if $\geq 75\%$ stenosis of the left main coronary artery, proximal left anterior descending artery, or at least two epicardial coronary vessels are present.²² In our study, we considered the presence of at least one epicardial coronary vessel stenosis $\geq 75\%$ for an ischaemic aetiology of HF. As already mentioned previously, magnetic resonance imaging is a precise non-invasive method distinguishing ICM from NICM. Its use as a gold standard to compare with 3D STE would be beneficial for obtained results validation. Due to the absence of data comparing rotational parameters in ICM and NICM, we could not perform a formal power analysis. Hence, we cannot exclude a difference in other rotational parameters if bigger cohort was investigated. Despite intra-observer and inter-observer reproducibility of the STE measurements were assessed, repeat echocardiograms for test/re-test reproducibility were not performed. The average frame rate of the 3D STE images was 18 Hz, which is the lower limit of acceptable temporal resolution. Finally, this is a pilot study, so the sample size is relatively small, and sensitivity and specificity of the AR threshold were not tested on a validation cohort.

Conclusions

In conclusion, our study showed that ICM is associated with higher values of AR compared with NICM. The cut-off value of 3.16° enables us to distinguish ICM and NICM and makes the AR a potential echocardiographic parameter of LV systolic dysfunction aetiology evaluation. This parameter assessed by 3D STE could be favourable in ascertainment of aetiology, risk stratification and so adequate treatment of HF patients. The great advantage of 3D STE is its relatively good availability, lower cost, time savings, and use of ultrasound beam instead of ionizing radiation. However, further validation of the AR is necessary in order to use it in clinical practice.

Acknowledgements

An independent research grant of the Ministry of Education, Science, Research and Sport of the Slovak Republic (VEGA 1/0338/17). An independent research grant of the Ministry of Education, Science, Research and Sport of the Slovak Republic (KEGA 030UK-4/2019).

Conflict of interest

Authors declare that there are no actual or potential conflicts of interest in relation to this article.

References

1. Minatoguchi S, Kawasaki M, Tanaka R, Yoshizane T, Ono K, Saeki M. Evaluation of systolic and diastolic properties of hypertensive heart failure using speckle-tracking echocardiography with high volume rates. *Heart Vessels* 2017; **32**: 1202–1213.
2. Kleijn SA, Aly MF, Terwee CB, van Rossum AC, Kamp O. Three-dimensional speckle tracking echocardiography for automatic assessment of global and regional left ventricular function based on area strain. *J Am Soc Echocardiogr* 2011; **24**: 314–321.
3. Maggioni AP, Dahlström U, Filippatos G, Chioncel O, Leiro MC, Drozd J, Fruhwald F, Gullestad L, Logeart D, Fabbri G, Urso R, Metra M, Parissis J, Persson H, Ponikowski P, Rauchhaus M, Voors AA, Nielsen OW, Zannad F, Tavazzi L, on behalf of the Heart Failure Association of the European Society of Cardiology (HFA). EURObservational Research Programme: regional differences and 1-year follow-up results of the Heart Failure Pilot Survey (ESC-HF Pilot). *Eur J Heart Fail* 2013; **15**: 808–817.
4. Sajeev CG, Rajan Nair S, George B, Rajesh GN, Krishnan MN. Demographical and clinicopathological characteristics in heart failure and outcome predictors: a prospective, observational study. *ESC Heart Fail* 2017; **4**: 16–22.
5. Ponikowski P, Voors AA, Anker SD, Bueno H, Cleland JGF, Coats AJS, Falk V, González-Juanatey JR, Harjola VP, Jankowska EA, Jessup M, Linde C, Nihoyannopoulos P, Parissis JT, Pieske B, Riley JP, Rosano GMC, Ruilope LM, Ruschitzka F, Rutten FH, van der Meer P, ESC Scientific Document Group. 2016 ESC Guidelines for the diagnosis and treatment of acute and chronic heart failure: the Task Force for the diagnosis and treatment of acute and chronic heart failure of the European Society of Cardiology (ESC) developed with the special contribution of the Heart Failure Association (HFA) of the ESC. *Eur Heart J* 2016; **37**: 2129–2200.
6. Korosoglou G, Giusca S, Hofmann NP, Patel AR, Lapinskas T, Pieske B, Steen H, Katus HA, Kelle S. Strain-encoded magnetic resonance: a method for the assessment of myocardial deformation. *ESC Heart Fail* 2019; **6**: 584–602.
7. Peterzan MA, Rider OJ, Anderson LJ. The role of cardiovascular magnetic resonance imaging in heart failure. *Card Fail Rev* 2016; **2**: 115–122.
8. Doh JH, Koo BK, Nam CHW, Kim JH, Min JK, Nakazato R, Silalahi T, Prawira H, Choi H, Lee SY, Namgung J. Diagnostic value of coronary CT angiography in comparison with invasive coronary angiography and intravascular ultrasound in patients with intermediate coronary stenosis: results from the prospective multicentre FIGURE-OUT study. *Eur Heart J* 2014; **15**: 870–877.
9. Lang RM, Badano LP, Mor-Avi V, Afilalo J, Armstrong A, Ernande L, Flachskampf FA, Foster E, Goldstein SA, Kuznetsova T, Lancellotti P, Muraru D, Picard MH, Rietzschel ER, Rudski L, Spencer KT, Tsang W, Voigt JU. Recommendations for cardiac chamber quantification by echocardiography in adults: an update from the American Society of Echocardiography and the European Association of Cardiovascular Imaging. *J Am Soc Echocardiogr* 2015; **28**: 1–39.
10. Galderisi M, Cosyns B, Edvardsen T, Cardim N, Delgado V, Di Salvo G, Donal E, Sade LE, Ernande L, Garbi M, Grapsa J. Standardization of adult transthoracic echocardiography reporting in agreement with recent chamber quantification, diastolic function, and heart valve disease recommendations: an expert consensus document of the European Association of Cardiovascular Imaging. *Eur Heart J Cardiovasc Imaging* 2017; **18**: 1301–1310.
11. Jafary FH. Devereux formula for left ventricular mass—be careful to use the right units of measurement. *J Am Soc Echocardiogr* 2007; **20**: 783.
12. Ibanez B, James S, Agewall S, Antunes MJ, Bucciarelli-Ducci C, Bueno H, Caforio ALP, Crea F, Goudevenos JA, Halvorsen S, Hindricks G, Kastrati A, Lenzen MJ, Prescott E, Roffi M, Valgimigli M, Varenhorst C, Vranckx P, Widimský P, ESC Scientific Document Group. 2017 ESC Guidelines for the management of acute myocardial infarction in patients presenting with ST-segment elevation: the Task Force for the management of acute myocardial infarction in patients presenting with ST-segment elevation of the European Society of Cardiology (ESC). *Eur Heart J* 2018; **39**: 119–177.
13. Wu VC, Takeuchi M. Three-dimensional echocardiography: current status and real-life applications. *Acta Cardiol Sin* 2017; **33**: 107–118.
14. Muraru D, Niero A, Rodriguez-Zanella H, Cherata D, Badano L. Three-dimensional speckle-tracking echocardiography: benefits and limitations of integrating myocardial mechanics with three-dimensional imaging. *Cardiovasc Diagn Ther* 2018; **8**: 101–117.
15. Tavakoli V, Sahba N. Assessment of age-related changes in left ventricular twist by 3-dimensional speckle-tracking echocardiography. *J Ultrasound Med* 2013; **32**: 1435–1441.
16. Cheung YF. The role of 3D wall motion tracking in heart failure. *Nat Rev Cardiol* 2012; **9**: 644–657.
17. Dalen VM, Geleijnse ML. *Left ventricular twist in cardiomyopathy*. InTech 2013: <https://doi.org/10.5772/55281> (22 May 2018).
18. Peteiro J, Bouzas-Mosquera A, Brouillon J, Sanchez-Fernandez G, Barbeito C, Perez-Cebey L, Martinez D, Vazquez-Rodriguez JM. Left ventricular torsion and circumferential strain responses to exercise in patients with ischemic coronary artery disease. *Int J Cardiovasc Imaging* 2017; **33**: 57–67.
19. Kroeker CA, Tyberg JV, Beyar R. Effects of ischemia on left ventricular apex rotation. An experimental study in anesthetized dogs. *Circulation* 1995; **92**: 3539–3548.
20. Haghighi ZO, Alizadehasl A, Moladoust H, Ardeshiri M, Mostafavi A, Rezaeiyan N, Ojaghi SH, Safi F, Mikaeilpour A. Left ventricular torsional parameters in patients with non-ischemic dilated cardiomyopathy. *Arch Cardiovasc Imaging* 2015; **3**: e26751 Accessed May 23th 2018.
21. McCrohon JA, Moon JC, Prasad SK, McKenna WJ, Lorenz CH, Coats AJ, Pennell DJ. Differentiation of heart failure related to dilated cardiomyopathy and coronary artery disease using gadolinium-enhanced cardiovascular magnetic resonance. *Circulation* 2003; **108**: 54–59.
22. Felker GM, Shaw LK, O'Connor CHM. A standardized definition of ischemic cardiomyopathy for use in clinical research. *J Am Coll Cardiol* 2002; **39**: 210–218.